Modeling and Characterization of a Propagation Channel in a Body-Centric Nano-Network

Charlie Pettersson (chpe0040@student.umu.se)

October 6, 2018

Abstract

Researchers have been trying to find smart health solutions that will allow people to continuously monitor their health through applications connected to the internet. One possible solution involve using nano-machines to create body-centric networks. However, the biggest challenge using nano-machines are how they would communicate with the outside world. To investigate this, I have in this thesis developed a multi-layer channel model for human skin tissues and investigated how signals at the terahertz frequency band interact with skin biomaterial. The model is built upon analytical equations describing electromagnetic propagation in a dielectric medium were the electromagnetic properties of human tissue were collected from different sources. The model were implemented in a flexible matlab program able to simulate different numbers of layers from a library with either fixed or random depths. The human skin model used to gather results were chosen to consist of 4 layers of epidermis, dermis, blood and hypodermis, and the depth of the layers were chosen to vary between typical values for the human body. This Matlab based multi-layer channel model was validated by a similar model made in CST Studio Suite, both for a single layer as well as for a 2-layer scenario. Results from the Matlab program showed that the path loss is significantly affected by frequency and material. The expected path loss could therefore vary significantly, however for a human skin model with depths of 1.23, 3.76, 0.21 and 1.38 mm respectively, the path loss was approximately between 250-350 dB for frequencies of 0.5-1.5 THz at the end distance. Finally, numerical analysis were used on 10 data sets created from the multi-layer channel model in order to develop a simple interpolation equation able to describe path loss through the human skin with varying tissue layer depths. The equation had an average mean error of 4.08 % and a maximum mean error of 6.61% against 90 different random data sets.

Contents

Acknowledgements

I wanna thank my supervisors at Ericsson, Gabor Fodor, Nafiseh Shariati and Hamed Farhadi for their guidance through this project. I also want to thank Bo Xu at Ericsson for his great help with CST Studio Suite. Furthermore I want to thank my supervisor at Umeå university Christian Larsen for his contribution to the report.

1 Introduction

Nowadays researchers are taking rapid steps toward reaching ubiquitous health solutions that will allow peoples health to be continuously monitored and accessible via the Internet. For example it could make it possible to detect diseases before they break out, drug dispensary could be automatic and one would be able to see it all in real time through a phone or other smart device. One of the promising research fields has been the one surrounding nano-machines. Researchers has been able to create machines that range from 10 up to 100 μm^2, these machines are able to perform simple tasks such as sensing, computation and actuation [1]. Abilities which makes these nano-machines highly desirable for many different purposes, but perhaps most importantly they could be used in the biomedical field. These nano-machines could perform continuous measurements of vital health parameters, deliver drugs at specific times or provide immune system support and due to its limited size they could access parts of the body it is otherwise dangerous to operate in [2]. One of the biggest concerns regarding the viability of these machines is how to solve their communication towards the outside world. Four different techniques have mainly been investigated, namely, molecular-, acoustic-, touch based- and electromagnetic communication [3].

For many years molecular communication seemed to be the more promising out of the four due to it already being a natural way of communication inside the body and the shortcomings of the other methods seemed far from being solvable. Touch-based- and acoustic communication did not produce results that were good enough and the size requirement of the antennas that would be used for electromagnetic communication were impossible to meet. But recent research in the field of graphene (and its derivatives carbon-nanotubes and -nanoribbons) has made it possible for researchers to create antennas just a few nanometers in size which has opened up the door for electromagnetic communication [4]. Due to the very limited size of these antennas they have very high resonant frequencies and the proposed frequency band therefore lays in the terahertz range (0.1-10 THz).

The terahertz frequency band has advantages such as that it is an unallocated frequency band which makes it possible to use ultrawide bandwidth communication schemes which in turn supports high bit rates in the range of Terabits per second [5], furthermore it is non-ionizing inside the body and not very susceptible to scattering effects. On the other hand one of the biggest drawbacks of this frequency band is that water molecules have very high absorption in this range due to experiencing rotational transitions[6]. This property has already caused terahertz radiation to be used in detection of skin cancer due to the small differences in water content it has compared to normal skin [7]. However in the case of wireless communication this causes a big problem since a human body consists of approximately 70% water. Another drawback of this frequency range is that it lies in the middle of optical and microwave frequencies and therefore there are no commercial terahertz transmitters or receivers today, which limits the number of measurements available.

Due to this, creating channel models can be difficult. Andrea Goldsmith a researcher on wireless communications at Stanford university said: "The complexity of signal propagation makes it difficult to obtain a single model that characterizes path loss accurately across a range of different environments." She also said, "it is sometimes best to use a simple model that captures the essence of signal propagation without resorting to complicated path loss models, which are only approximations to the real channel anyway."

Channel models are traditionally derived from complex ray tracing models or empirical measurements when specific system requirements have to be met [8]. But due to the complexity of the human body and the unavailability of measuring equipment both of those methods are hard to perform. Therefore the current research done on the field has focused on analytical models based on common wireless communication concepts [6], [9] or different numerical models trying to approximate the behaviour of human tissue at these frequencies [10], [11].

The rest of this paper is organized as follows. In Section 2 the goals of the thesis and the objectives set up in order to achieve those goals are described. Thereafter Section 3 will show all the relevant theory used in order to calculate the path loss in human tissue. Section 4 describes the method used for creating the channel model, how the validation of the channel model were done, describing how the human skin model were chosen as well as how polynomial regression were used to find a simple equation describing the path loss. After that, section 5 shows the relevant results of the channel model, Section 6 discusses the channel model and its results and finally a short conclusion is held in Section 7.

2 Objectives and Goals

This thesis is Ericssons first project on the topic of in-vivo electromagnetic communication between nano-machines. The purpose of this paper is thus to gain a deeper knowledge of the topic and also to create a self made tool for evaluation of the possibility of communication between such devices. The end result should be in the form of an equation that models the path loss of an electromagnetic signal traversing the human skin at terahertz frequencies. In order to reach this goal the objectives of this thesis are to

- Get a broader understanding by reading up on the current research regarding nano-machines and path loss models inside human tissue in the terahertz frequency band.
- Re-implement some of the earlier results produced by other researchers to get a better understanding of in vivo terahertz channel models.
- From previous results, make a matlab based program able to simulate path loss through a dispersive medium and include the option to simulate through multiple layered mediums to characterize the whole channel.
- Simulate a stack of mediums that as accurately as possible represents the human skin, in order to find how difficult it would be to bring information in and out of the body.
- Make a model in CST microwave studio that can be used as a reference to check the validity of the program.
- Finally by using the program create a large number of data sets that can be used to derive an interpolation model in order to get a simple equation that represents the path loss of a signal propagating in or out of the skin.

3 Theory

The following chapter will be divided in three parts, where the first describes the equations used for the actual channel, the second describes the theory used to display the electromagnetic properties of human tissue and the last chapter show the equations used for calculating the path loss used for validation.

3.1 Path Loss Model

The total path loss experienced by a electromagnetic wave propagating through a dispersive medium can be expressed as

$$PL_{tot}[dB] = PL_{spr}[dB] + PL_{abs}[dB] + PL_{sca}[dB]. \tag{1}$$

Where PL_{spr} is the path loss due to spreading, PL_{abs} is the path loss due to absorption and PL_{sca} is the path loss due to scattering.

The path loss due to spreading is not a loss per se, it can more accurately be described as a thinning of information when a wavefront is propagating in space. When an electromagnetic wave travels in a dielectric material some of the power from the wave will be absorbed in the material which causes vibrations and as such some of the information will be lost as heat. There are different kinds of scattering depending on the relative size of the material molecules and the wavelength of the electromagnetic wave. In the case of terahertz frequencies the wavelength is bigger than most molecules found in the body which means that Rayleigh scattering will occur. This means that since the wavelength is so large the molecule will see the wave as a constant electric field which will cause a dipole to occur in the molecule, this dipole will in turn start to oscillate with the electromagnetic wave which makes the dipole radiate power in the form of scattering. It has been shown in previous studies that the effects of scattering is negligible in the terahertz range compared to the other path loss factors [6] and we can simplify eq.(1) as,

$$PL_{tot}[dB] = PL_{spr}[dB] + PL_{abs}[dB]. \tag{2}$$

Furthermore as we move from a single medium to a stratified media stack we also have to include losses due to reflection in interface boundaries and the equation can thus be written as

$$PL_{tot}[dB] = PL_{spr}[dB] + PL_{abs}[dB] + PL_{ref}[dB], \tag{3}$$

where PL_{ref} is the reflection path loss. The spreading path loss can be expressed by the famous Friis transmission formula which relates the free space path loss, antenna gains and wavelength to the received and transmit powers, it is characterized as

$$PL_{spr} = D\left(\frac{\lambda_g}{4\pi d}\right)^2. \tag{4}$$

Here D is the directivity of the transmitting antenna relative to an isotropic antenna, d is the distance the wave has traveled. The effective wavelength can be derived as $\lambda_g = \lambda/n'$ where n is the refractive index of the medium which can be divided into its complex parts as $n = n' - n''$. The directivity refers to the maximum gain of the antenna and can be calculated by dividing the maximum power density, $P_{max}(\theta, \phi)$, by its average,$P_{av}(\theta, \phi)$, over a sphere observed in the far-field of the antenna, i.e.

$$D = \frac{P_{max}(\theta, \phi)}{P_{av}(\theta, \phi)}. \tag{5}$$

The attenuation due to absorption of an electromagnetic wave passing through a dispersive medium can be calculated from the Beer-Lambert law as,

$$PL_{abs} = e^{-\mu_{abs} d}. \tag{6}$$

Where μ_{abs} is an attenuation coefficient due to absorption of the dispersive medium that depend on the specific light absorbing molecules in the medium. It was first dervied and computed for gas particles by [5], the same approach can be used in the body as well due to the nanoscale structures of human tissue. The coefficient can be calculated as

$$\mu_{abs} = \frac{4\pi n''}{\lambda}. \tag{7}$$

The reflection losses at the interface boundaries can be calculated by using the Fresnel equations for non-magnetic medium since human tissues has been shown to have no magnetic properties in the terahertz region [6]. By assuming normal incidence the reflection can be described by

$$PL_{ref} = \left(\frac{n_1' - n_2'}{n_1' + n_2'}\right)^2, \tag{8}$$

with n_1' and n_2' being the refractive index of the medium the wave is propagating from and to, respectively.

3.2 Dielectrics

Human tissue acts as a dielectric which means that it cannot carry charge like a metal does, but electric fields can still propagate through it. This means that we can display the complex permittivity of human tissue as,

$$\epsilon_r = \epsilon_r' - i\epsilon_r''. \tag{9}$$

Since human tissue has no magnetic properties, the magnetic permeability μ_r is approximately equal to unity and the refractive index can be simplified as

$$n = \sqrt{\epsilon_r \mu_r} \approx \sqrt{\epsilon_r}. \tag{10}$$

The human tissue consists of biomedical nano-structures that most prominently is water molecules, so to accurately model the needed material properties at the terahertz frequency band different approximations of dielectric relaxation can be used. The Debye model is the simplest of those models and is stated as,

$$\epsilon_r = \epsilon_\infty + \sum_k \frac{\Delta\epsilon_k}{1 + i\omega\tau_k}. \tag{11}$$

Here k signifies each different relaxation process, ϵ_∞ is the permittivity at the high frequency limit, $\Delta\epsilon$ is the permittivity difference between each relaxation process (for only one process $\Delta\epsilon = \epsilon_s - \epsilon_\infty$, where ϵ_s is the static permittivity at the low frequency limit), τ is the characteristic relaxation time relating to that specific process and $\omega = 2\pi f$ is the angular frequency. The Debye model can be rationalized to its real and imaginary parts as

$$\epsilon_r' = \epsilon_\infty + \frac{\Delta\epsilon_k}{1 + (\omega\tau_k)^2}, \tag{12}$$

$$\epsilon_r'' = \frac{\Delta\epsilon_k(\omega\tau_k)}{1 + (\omega\tau_k)^2}. \tag{13}$$

Another variant of the Debye model is the Havrilak-Negami model that takes into account the asymmetry and broadness of the dielectric dispersion curve.

$$\epsilon_r = \epsilon_\infty + \sum_k \frac{\Delta\epsilon_k}{(1 + (i\omega\tau_k)^\alpha)^\beta} - j\frac{\sigma}{\omega\epsilon_0}, \tag{14}$$

where σ is the ionic static conductivity, $\epsilon_0 \approx 8.854 \cdot 10^{-12}$ Fm^{-1} is the free space permittivity and α and β is heuristically derived power law exponents. The Havrilak-Negami model can also be rationalized into its real and imaginary parts as,

$$\epsilon_r' = \epsilon_\infty + \Delta\epsilon_k(1 + 2(\omega\tau_k)^\alpha \cos(\frac{\pi\alpha}{2}) + (\omega\tau_k)^{2\alpha})^{-\beta/2} \cos(\beta\phi_k) \tag{15}$$

$$\epsilon_r'' = \Delta\epsilon_k(1 + 2(\omega\tau_k)^\alpha \cos(\frac{\pi\alpha}{2}) + (\omega\tau_k)^{2\alpha})^{-\beta/2} \sin(\beta\phi_k) - \frac{\sigma}{\omega\epsilon_0}. \tag{16}$$

with ϕ_k being a constant defined as,

$$\phi_k = \arctan\left(\frac{(\omega\tau_k)^{\alpha_k} \sin(\pi\alpha_k/2)}{1 + (\omega\tau_k)^{\alpha_k} \cos(\pi\alpha_k/2)}\right). \tag{17}$$

3.3 Instantaneous Power

In order to calculate the instantaneous power received by an antenna we define

$$P = P_{density} A_e, \tag{18}$$

where $P_{density}$ is the power density and A_e is the effective aperture of the antenna. The power density in a point of the propagating wave can be calculated from

$$P_{density} = \frac{|E|^2}{2Z}, \tag{19}$$

where E is the electric field, $Z = Z_0\sqrt{\mu_r/\epsilon_r}$ is the wave impedance, with $Z_0 \approx 377\ \Omega$ as the free space wave impedance. Furthermore the effective aperture of an infinitely small antenna is described by,

$$A_e = \frac{\lambda^2}{4\pi}. \tag{20}$$

We can then use eq. (18) to calculate the path loss for a propagating wave at an arbitrary point compared to the power of the transmitting antenna, $P_{antenna}$, as

$$PL = \frac{P}{P_{antenna}}. \tag{21}$$

4 Method

As mentioned earlier, the goal of this thesis is to describe the communication between an in vivo nano-machine and an out of body wearable, a schematic picture of the intended user case can be seen in Figure 1. The overall method of reaching this goal is thus divided into 4 different steps. First the primary constituents of human skin was found and what types of tissue we could use for our simulation. Second a path loss model was created in matlab, which originally was very restricted in what it could do, but were expanded throughout the whole project. Third the solutions provided by the program were compared against the solution from a similar model created in the software CST Studio Suite. Finally after the program had been validated the data created were used in numerical analysis to create a simple equation able to describe path loss of an electromagnetic wave passing through any human skin at terahertz frequencies.

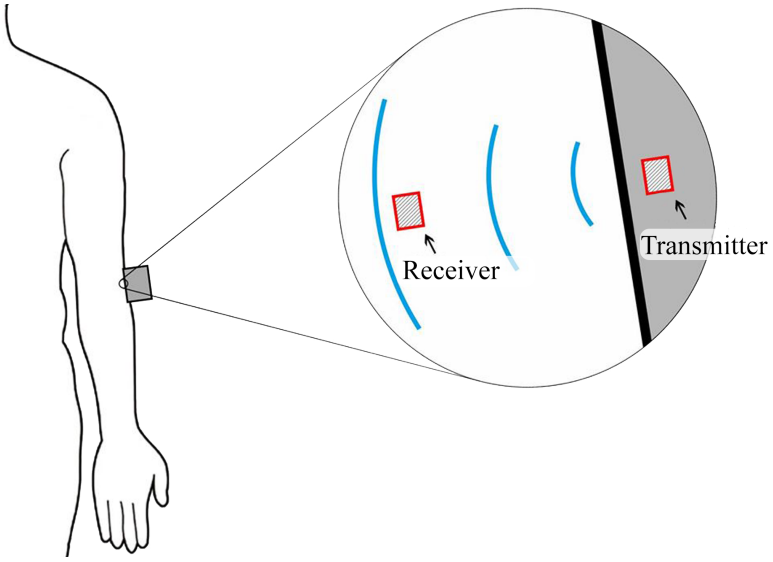

Figure 1: A schematic picture displaying the intended user case where a nano-machine communicates with an outside node located in a wearable.

4.1 Electromagnetic Properties of Human Tissues

The parameters used to calculate the permittivity of different human tissue can be found in Table 1 which contains values collected from multiple sources found in available literature. The parameters have either been used in the Debye relaxation model for two relaxations processes or the Havrilak-Negami model for one or two relaxation processes. What kind of method is used for each tissue can be seen by the number of available parameters for that specific tissue. The tissues found in the table are all calculated from measurements that focus on the 0.5-1.5 THz interval due to the restrictions of the current measurement setups.

By whole blood it means the whole mixture that is typically donated when performing a blood transfusion. It contains about 55 % red blood cells and 45 % blood plasma and a small amount of white blood cells. As such it do not accurately represent the entire blood vessel which also contains vessel walls that contain the blood. The values for skin was calculated when trying to determine differences between normal skin and skin with cancer, it thus represent a generic piece of averaged out skin while the other remaining parameters, i.e. stratum corneum, epidermis, dermis and hypodermis is the main constituents of skin. The epidermis is the outermost layer of the skin and is responsible for keeping infective pathogens out of the body and water content inside of it. It is subdivided into 4 (5 in the palms and soles of the foot) layers with different functions. The stratum corneum is the outermost layer of the epidermis which contains 10-30 layers of dead keratinocytes that is continously shedding, it is therefore the thoughest layer of the skin. Below the epidermis lies the dermis which primary job is to relieve the body of stress and strain, its main constituents are collagen and elastic fibers. Unlike the epidermis, the dermis contains many other type of cells such as blood vessels, sweat glands, hair follicles, lymph glands and nerve endings. The hypodermis is the innermost layer of the skin which purpose is to act as an insulator and

Table 1: Parameter values for the permittivity approximations.

Parameter	Water	Whole Blood	Skin	Stratum Corneum	Epidermis	Dermis	Hypodermis
α_1	-	-	-	1	0.95	0.92	1
α_2	-	-	-	-	-	0.97	0.89
β_1	-	-	-	1	0.96	0.8	0.78
β_2	-	-	-	-	-	0.99	0.90
τ_1 (ps)	8.4	14.4	10.6	15.9	15.9	1.6	2.3
τ_2 (ps)	0.1	0.1	0.2	-	-	159 (ns)	15.9 (ns)
$\Delta\epsilon_1$	74.3	126.2	56.4	12.22	89.61	5.96	1.14
$\Delta\epsilon_2$	1.2	1.7	0.6	-	-	380.4	9.8
ϵ_∞	3.3	2.1	3.0	2.4	3	4	2.5
σ (S/m)	-	-	-	0.035	0.01	0.1	0.035
Source	[12]	[13]	[12]	[11]	[11]	[11]	[11]

shock absorber for the inner organs of the body, it is also where the body stores energy in the form of fat.

To simulate a signal going in and out of the body a human skin model is needed. The human skin is a very complex organ with multiple constituents to its structure which was impossible to accurately display in the model, mainly due to the shapes and functions of the structures but also because of the unavailability of permittivity measurements. It was therefore decided that the model would have the 4 layers of epidermis, dermis, whole blood and hypodermis, in that order (see Figure 2). That way we keep the model as simple as possible whilst still keeping the most important parts of the human skin. The thickness of the 4 different layers typically ranges from 0.05-1.5 mm for the epidermis, 1.5-4 mm for the dermis and 0.1-1.5 mm for the blood vessels. The hypodermis on the other hand can vary by a lot between different humans and do not have a typical value.

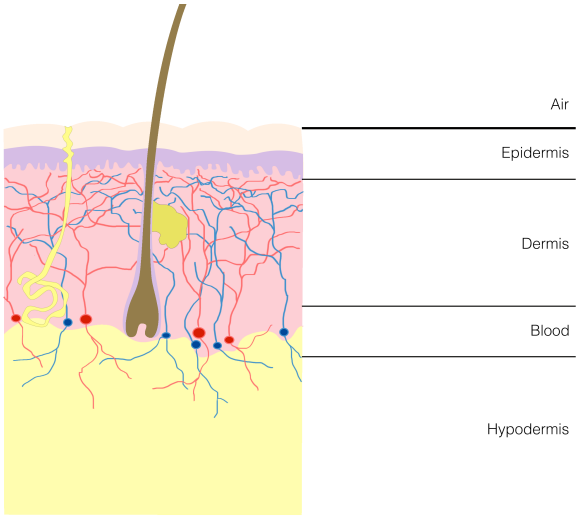

Figure 2: A picture showing the complex structure of the human skin (left) versus the simplified version used in the simulations (right).

4.2 Matlab Based Path Loss Program

The matlab path loss program is based upon eq.(3-17) and could initially only calculate path loss through a single layer. But in order to characterize the entire channel through the human skin the model was changed to consider the channel as a stratified media stack with different electromagnetic properties. If a multi-layer model where to be simulated without any alterations there would be

discontinuous parts in the solution since the equations do not take into account what has happened to the signal previously, but only shows the curve corresponding to that specific medium at that specific distance. To account for this, the difference between the last point in each layer and the first in the next where computed and multiplied into the next layer to make the curve continuous. This difference had to be calculated cumulative for each subsequent layer after the second in order to keep all layers continuous.

Because this is a multi-layer model the reflection described by eq.(8) also has to be taken into account in the interface boundaries. This was easily added in since the previously mentioned discontinuities had been dealt with.

In order to have a simple and flexible program that could easily simulate different layers a material library were created that contained the parameter values found in table 1 and the corresponding equations to solve the permittivity of each tissue type. Thereafter a text file could be used to call upon the model with multiple layers and different depths of these layers. A function was also added in with the possibility of having the layer depths being randomized between typical values for those layers [14]-[16] which were used in order to quickly create many data sets used for the numerical analysis.

4.3 CST Studio Suite

CST Studio Suite is a electromagnetic simulation software which can solve problems for a wide range of frequencies, everything from low frequency to optics. It also has solvers for some mechanical and thermal problems. The suite comes with many different studios that each has specialized tools for different types of problems.

The microwave studio module, which is good at producing fast and efficient solutions to high frequency problems with its time-domain solver, was used to create the reference models for validation of the matlab program. The model consists of an ordinary half wave dipole antenna, which can be seen in Figure 3, that produces signals with a directivity of approximately 2.15 dBi [17]. A half wave dipole antenna was used since it is one of the most common antennas and also simple to create. The length of the antenna was set as $143{\cdot}10^6$ divided by the frequency or as the name suggests, approximately half of the wavelength. The gap between the two antenna rods where 1/200 of the length, the radius of the rods where 1/1000 of the wavelength and the impedance of the antenna was set to 73 Ω [18].

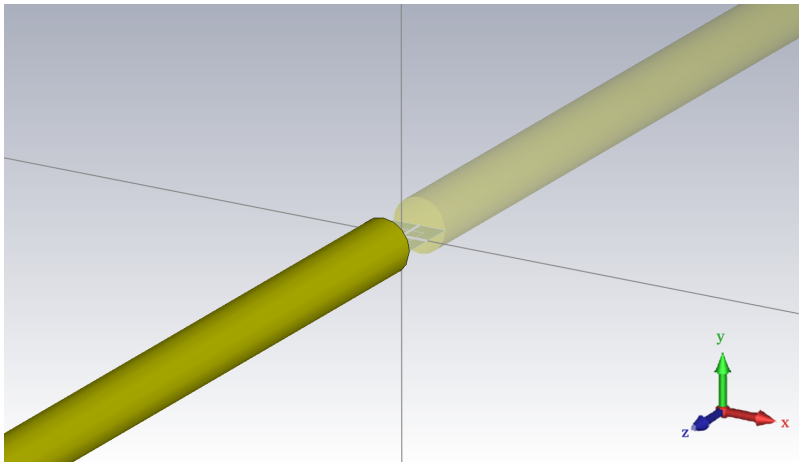

Figure 3: A picture displaying the antenna modeled in CST microwave studio.

Around the antenna, a cube of dispersive medium was placed with the dimensions of 1.0 x 1.0 x 1.0 mm^3. The cube (can be sen in Figure 4a) were chosen to have the material parameters of epidermis (see Table 1 and equations eq.(15) and (16)) and the boundary conditions of the cube were set as perfect matched layers, which means that they absorb all electromagnetic radiation and reflects nothing back into the geometry. The antenna was placed in the z-direction and it therefore radiated in both the x- and y-direction where electric field probes where placed with 0.05 mm increments up to the boundary of 0.5 mm in order to calculate the instantaneous power at these locations with equation eq.(18-21). Models were made for antennas at 0.5, 1 and 1.5 THz for comparison with the matlab program. In order to test the multi-layer properties of the matlab

program another model was also created. This model was similar in every regard to the last, but contained a sphere of dermis in the center, closest to the antenna, (see Figure 4b) of radius 0.25 mm.

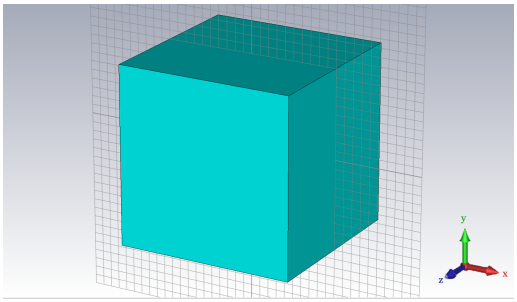

(a) The geometry of the single layer validation.

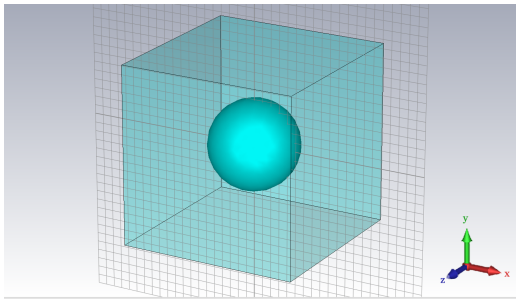

(b) The geometry of the 2 layer validation.

Figure 4: The two different geometries used in CST for validation. Figure 4a shows the cube with side 1 mm with material parameters of epidermis. Figure 4b has a sphere with radius 0.25 mm with material parameters of dermis, surrounded by the same cube as in 4a.

4.4 Polynomial Regression

To perform the polynomial regression 10 datasets from the matlab path loss program were run through a multidimensional polynomial regression function. This in turn created 10 individual polynomials whose coefficients were averaged out against one another to create a single polynomial. The polynomials were set to be of the 4th order and and was based on 2 dependent variables, the frequency and the distance. The datasets used for the polynomial regression was based on a human skin model with a constant total depth of 6.6 mm. The values were randomized between 0.5-1.5 mm for epidermis, 3-4 mm for dermis and 0.5-1 mm for blood. The hypodermis layer was set as the remainder to fill up the constant depth, i.e. between 0.1-2.6 mm. This was done in order to simulate some of the thicker skin found on the body such as on the arms or the torso where we are most likely to have wearables connected to these devices. In order to test the accuracy of the polynomial 90 other data sets with the same constraints for the tissue depths were created as a reference.

5 Results

By using the values from Table. 1 and the respective equation of either eq.(12,13,15,16) the permittivity can be calculated for frequencies between 0.5-1.5 THz. The real part of the permittivty of the four layer human skin model can be seen in Figure 5a, while the imaginary part of the permittivity for the same layers can be seen in Figure 5b.

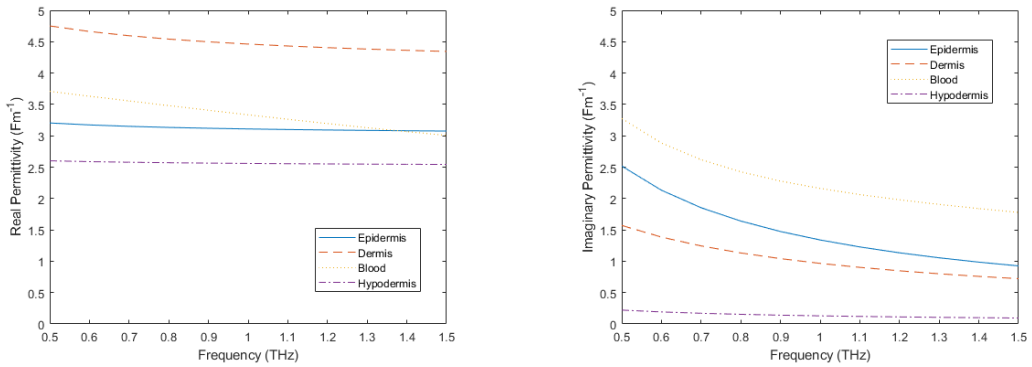

(a) Real part of the permittivity.

(b) Imaginary part of the permittivity.

Figure 5: Real and imaginary part of the frequency dependent permittivity for the 4 layers in the human skin model.

Figure 5a and 5b contains the information that describes how electromagnetic waves behave in this frequency range for these specific tissues. The variations between the lines will characterize the difference in the path losses seen in Section 5.2.

5.1 Validation

To make sure that the solutions provided by the matlab program is accurate the total path loss was compared to the solution of the CST Studio Suite model. The path loss from CST was calculated using eq.(18-21) and was compared to the total path loss computed through the matlab program. Comparisons between the two in a layer of epidermis can be seen for 0.5, 1.0 and 1.5 THz in Figures 6a-6c respectively.

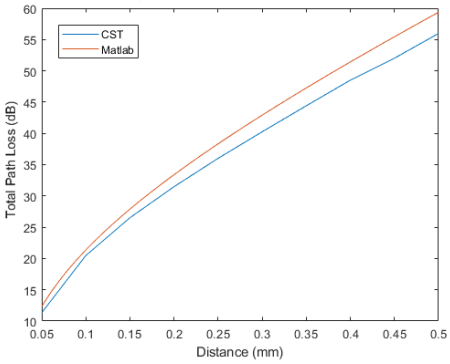

(a) The total path loss at 0.5 THz for a single layer of epidermis.

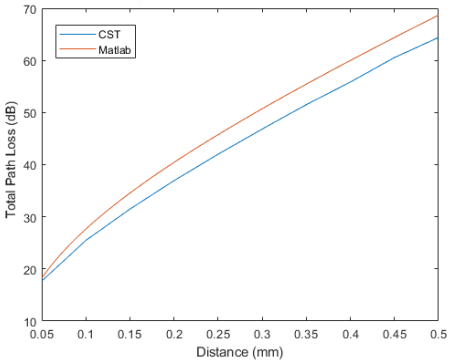

(b) The total path loss at 1.0 THz for a single layer of epidermis.

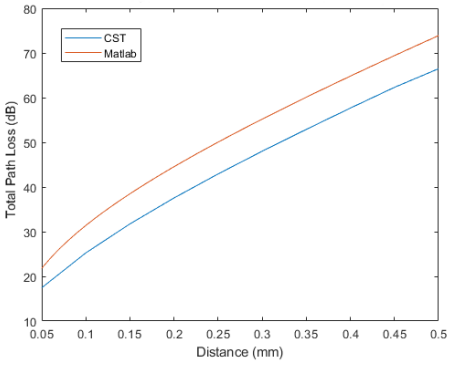

(c) The total path loss at 1.5 THz for a single layer of epidermis.

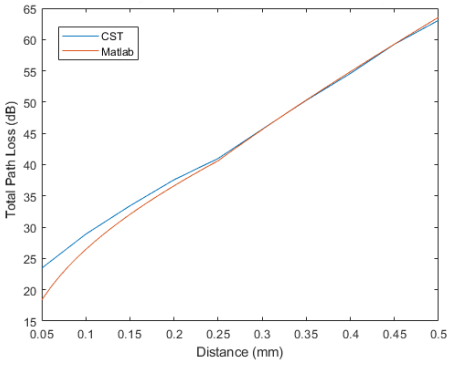

(d) The total path loss at 1.0 THz for the 2 layers of dermis and epidermis.

Figure 6: Comparison of the total path losses between the model created in CST microwave studio and the matlab based program. Figure 6a, 6b and 6c are the results for a single layer of epidermis at 0.5, 1.0 and 1.5 THz respectively and Figure 6d are for a 2 layer model of dermis and epidermis at 1.0 THz

.

It appears that for all 3 single layer cases the lines has the same shape, but there seems to be an increasing error between for the higher frequencies. It is worth noting that this error does not seem to increase with distance which is seen most notably in Figure 6c. The results for a multilayer path loss can be seen in Figure 6d where a layer of dermis were placed before the epidermis. Here we see that the CST solution seems to have the higher path loss initially whilst in the other cases it was the other way around. We can also see that after the interface boundary the two lines seems to follow very closely.

5.2 Path Loss Model

For the results below a human tissue model with randomized tissue depths were used as explained in Section 4.3. The depths was 1.23 mm for epidermis, 3.76 mm for the dermis, 0.21 mm for the blood and 1.38 mm for the hypodermis, which results in a total depth of 6.58 mm. With the permittivities in Table 1 the path losses could now be calculated. The spreading path loss across all distances for 0.5, 1.0 and 1.5 THz can be seen in figure 7.

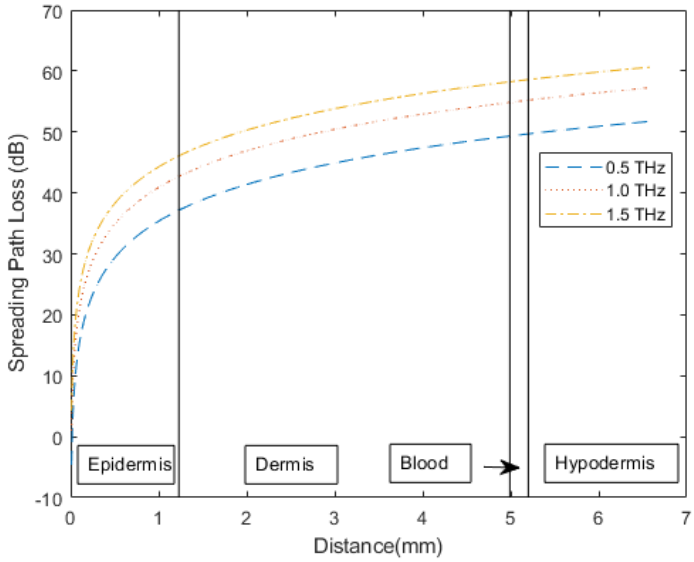

Figure 7: The spreading path loss against distance at 0.5, 1.0 and 1.5 THZ for the 4 layer human skin model.

The spreading path loss does not seem to be very material dependent, in fact it only differ by a few dB when compared for different materials side by side over large distances. By using the frequency dependent imaginary permittivity in Figure 5b combined with eq.(7) the absorption coefficient for the 4 different layers were found which can be seen in Figure 8.

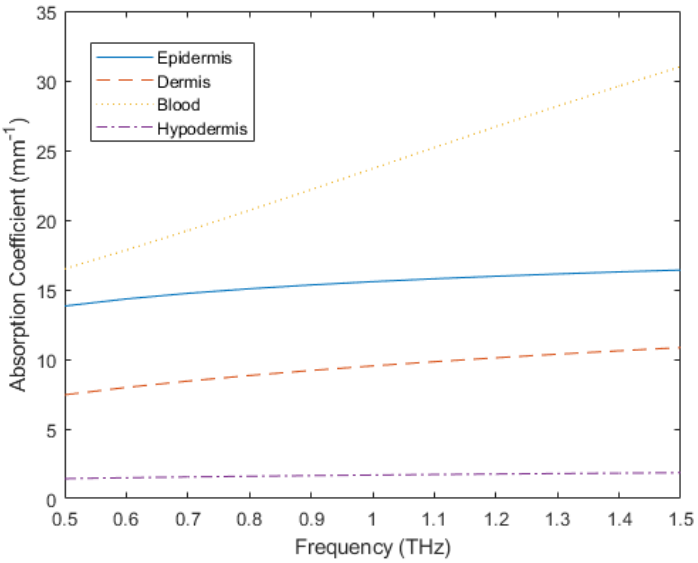

Figure 8: The frequency dependent absorption coefficient of the 4 layers in the human skin model.

With the absorption coefficient the path loss due to absorption can be found with eq.(6) and can be seen against all distances for frequencies of 0.5, 1.0 and 1.5 THZ in Figure 9.

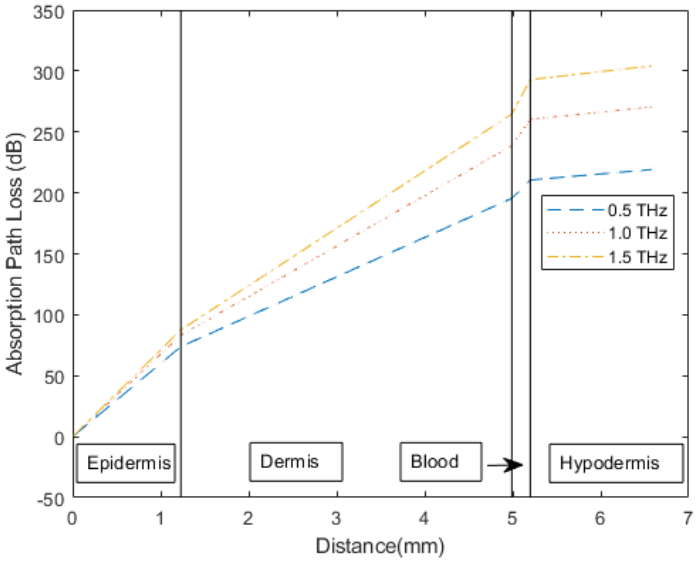

Figure 9: The absorption path loss against distance at 0.5, 1.0 and 1.5 THz for the 4 layer human skin model.

As mentioned earlier in Section 1, the absorption path loss is much higher than that of spreading and we see clear differences between the different tissues. We can also see that blood seems to suffer from the highest amount of attenuation, followed by epidermis, dermis and hypodermis in that order, which is what we would suspect when thinking of the amount of water content in each tissue. The reflection at the interface boundaries of the layered model was calculated using eq.(8) and can be seen in Figure 10.

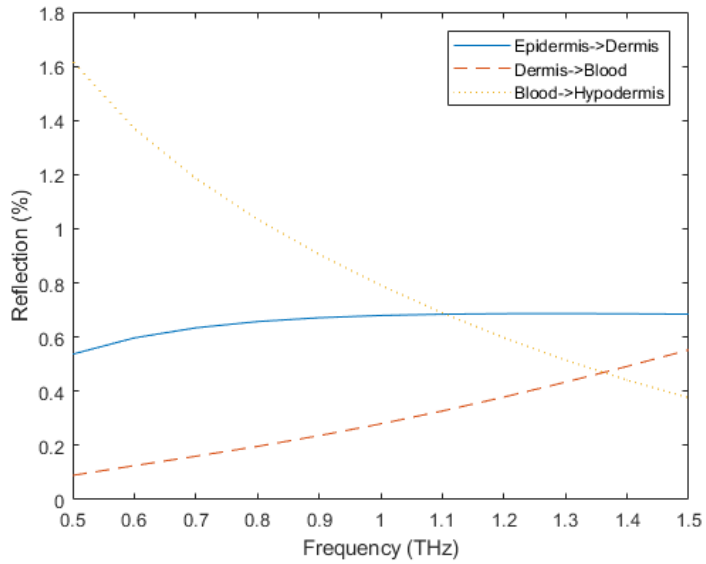

Figure 10: The frequency dependent reflection displayed in % for the 3 different interfaces of our 4 layered human skin model.

The reflection for these specific boundaries reached a maximum of 1.6 % which amounts to a loss of less than 0.1 dB. Finally by adding together all losses according to eq.(3) the total path loss can be seen against all frequencies and distances in Figure 11.

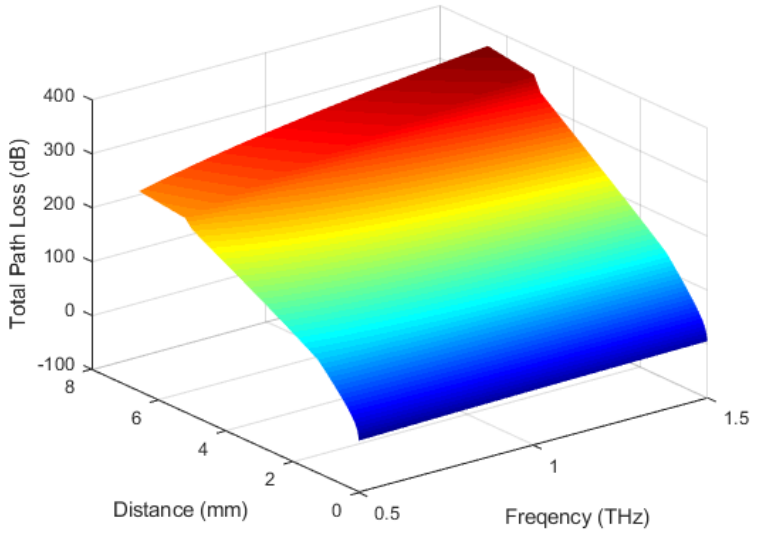

Figure 11: The total path loss against both frequency and distance for the 4 layer human skin model.

From Figure 11 we see that the total path loss for a electromagnetic signal traveling through a randomized human tissue stack of depth 6.58 mm seems to suffer between 300-375 dB for the frequency range 0.5-1.5 THz.

5.3 Polynomial Regression

The 15 coefficients corresponding to the 4th order polynomial mentioned in Section 4.4 can be seen in Table 2.

Table 2: 4th order coefficients for the two dimensional polynomial.

d^4	-0.7475	d^3f	-0.2915	d^3	10.2665
d^2f^2	0.7177	d^2f	2.6268	d^2	-48.0738
df^3	2.5147	df^2	-17.3197	df	29.4830
d	110.9589	f^4	-15.5318	f^3	70.7033
f^2	-118.0479	f	96.8260	Constant	-19.0850

The evaluation of the 4th order 2-dimensional polynomial can be seen in Figure 12a. The polynomial was evaluated in the same points as the data sets it was created from for easy visual evaluation.

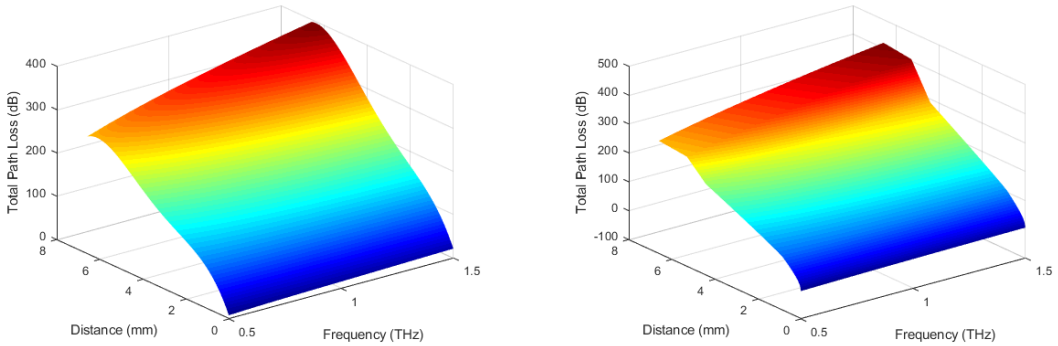

(a) The polynomial evaluated in the same points as the data sets it was created from.

(b) One of the data sets used to create the polynomial in Table 2.

Figure 12: A side by side comparison of the evaluation of the polynomial found in Table 2 and one of the data sets used to create it and subsequently it tries to model.

It appears that the polynomial in Figure 12a holds a similar appearance as the total path loss showed in Section 5.2 and the R2 and R2-adjusted value of the polynomial regression was both 0.9919. But when compared to a random data set found in Figure 12b we see significant differences especially in the interface boundaries. The frequency of the actual differences in each point between the two figures can be seen in Figure 13.

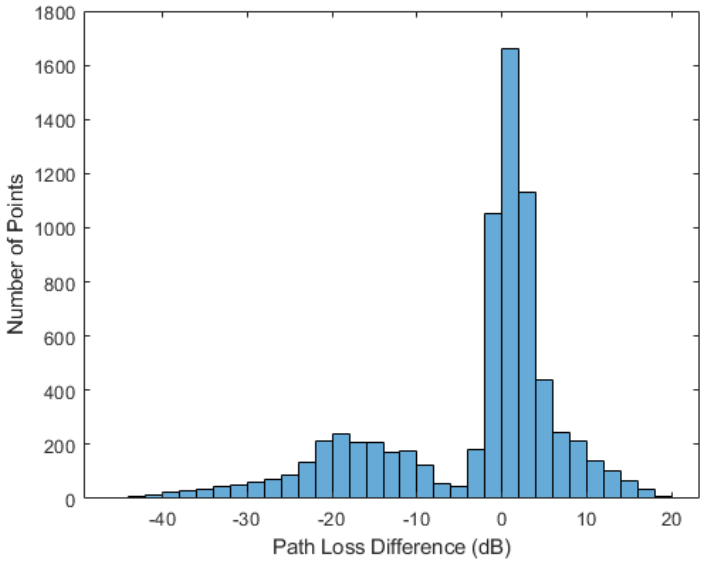

Figure 13: A histogram showing the frequency of the actual difference in each point between the two total path losses in Figure 12.

It can be seen that the actual differences is mostly centered close to 0 (which explains the good R2 and R2-adjusted values), but it can also be seen that it varies by as much as -40 to +20 dB for this specific data set. The mean difference between the polynomial and a random data sets was calculated and can be seen for 90 different data sets in Figure 14.

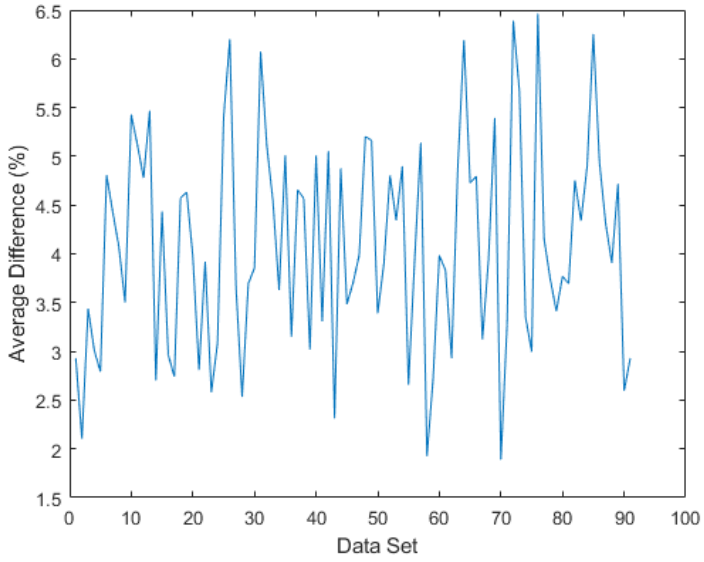

Figure 14: The average difference across all points between the polynomial and 90 other random data sets.

The mean difference across all 90 data sets were found as 4.08 % and the maximum mean difference against any data set were 6.61%.

6 Discussion

Due to the limited available terahertz transmitters we have today there are very few measurements done in this frequency range. Which in turn has a direct impact on the quality of this work. If there were more data available, more accurate permittivity models could have been used and more tissues could have been included in the material library. This is also the cause for using CST Studio Suite as the validator. It would have been of interest to actually take a measurement (in some capacity, measuring through the skin has it's own set of challenges) to compare against. There would also be the possibility of creating a deterministic channel model from many such data sets and see how that would compare with this model.

Using CST as a validator worked fairly well considering that due to the high frequencies investigated, the mesh of the geometry was very fine which in turn limited the space we could consider for our model to only 0.5 mm in each direction. The results are close enough that the matlab program can be fairly trusted. CST uses Maxwell's equations to calculate the wave propagation numerically whilst the matlab program uses analytical expressions that are not connected to Maxwell's equations so some differences are likely to occur. As for the differences seen in figures (6a-6c), since the shape of the curves were so similar, the error did not increase in distance but increased with frequency it is most likely a cause of the mismatch between the different antennas used in the programs. In matlab I assume that we have a half-wave dipole antenna with 2.15 dBi gain while in CST I had to design my own. For the multi-layer comparison, the two curves were very close in similarity at the further distances which show some promise of the model, although the fact that the models switched places for low distances is peculiar since you would expect that they would behave the same as in the single layer case except for potential reflections at interface boundaries which were shown to be very minor. It should also be noted that the choice of using a half wave dipole antenna was merely due to its simplicity and was simply used for comparison purposes and is not used by any nano-antennas to my knowledge.

As for the matlab program it has to be highlighted that the model is an oversimplification in many different ways. The human skin is far more complex than what we consider here with all of the different constituents of skin such as hair follicles, glands, network of capillaries and even sweat ducts have been shown to have electrical properties affecting the propagation of electromagnetic waves[10]. Using the measurement of whole blood to define a blood vessel is probably not very realistic either as the vessel walls are quite elastic and would contain more skin like features than

the very aquatic whole blood. These differences however does not affect the comparison between the matlab program and CST, just against the actual solution. The model do not consider any kind of multi-path opportunities, only a signal propagating in a straight line with full losses in the interface reflections. The model also assumes that the direction of the antenna is always facing outwards from the skin. This might not be very probable if the machines are diffusing inside the human body, unless we consider a large network of nano-machines were the possibility of always one being in the right direction increases. All of these effects are probably minor, but all add to the non-realism of the model.

The purpose of doing a numerical analysis was to find a simple equation that was easy to "carry around" and would not need any softwares to quickly find an answer to a path loss problem anywhere on the human skin. It should be noted that the need for an equation otherwise is unnecessary since the answers from the matlab based program is exact in the way that you will get the same answer every time given the same conditions. I choose to keep the polynomial at the 4th order since increasing the order did not significantly increase the accuracy of the polynomial and by going down to a 3rd order model the average error almost doubled. Similarly the choice of using 10 data sets was also based on accuracy, there were no significant changes when I tried increasing the value to 20 or 30 and therefore 10 seemed sufficient. The choice of limiting the tissue depths served in our favor in the way that by restricting the variance of the outputs the likelihood that the 10 curves used for the polynomial were more similar to another random data set. This means that the more narrow the tissue depths the better the accuracy of the polynomial would become, but at the same time it would defeat the purpose of being used anywhere at the human skin. This is why the focus ended up being the more thick skin that was most likely to represent how an actual scenario would look like. The polynomial ended up with having a mean error across 90 data sets of 4.08 %, but the actual differences could be upwards 40 dB in a single point which is too much for any reliable data to be extracted. The lack of time is the reason why only a multi-dimensional polynomial regression were done as the numerical analysis tool. A better method of interpolation would make the final result a lot better, preferably a method that would take into account the depth of each specific layer and not just the total depth.

One of the big reasons for using terahertz frequencies is the fact that the frequency band is unallocated and therefore could support very high capacities if the whole envisioned band could be used (0.1-10 THz). Although all of the current measurements are focused around the low terahertz band (0.1-2 THz). It would be interesting to investigate what happens at higher terahertz frequencies as well, especially since it has been shown that water molecules experience hindered longitudinal and rotational motion in these regions [19] which would alter its dielectric properties. The complete knowledge of the entire frequency band would help realize this technology. Another interesting aspect to evaluate would be to investigate if the heat expulsion due to the high absorption in human tissues follows current safety regulations, since heating could have severe effects on the human body and to my knowledge only one article has investigated it so far [20].

As for the actual results of this thesis it is clear that the conditions for wireless communications inside human tissue at terahertz frequencies is absolutely horrendous with attenuations of several hundred decibels after only a few millimeters. This reinforces the idea of having multiple nano-machines creating a body centric nano-network in order to bring out a signal. Not only that, but there need to be thought through, rigorous physical layer algorithms in order to realize this technology.

7 Conclusions

In this thesis a channel model for terahertz communication in human skin was proposed by considering spreading, absorption and reflection as different independent losses. The model was furthermore validated by comparing solutions to another model created in CST studio suite.

Overall I think the model does very well what was intended of it. It characterizes the entire channel out of the skin in a simple way and is built in a versatile manner which opens up the possibility of adding more complexity or use cases for it. It serves as a great starting point into the understanding of in-vivo channel models and nano-communication. As for the polynomial interpolation I do not think it is accurate enough that it could be used for any practical situations, but it gives a broad feel of how the path loss in human skin looks like at these frequencies.

References

[1] I.F. Akyildiz and J.M. Jornet, *"Electromagnetic wireless nanosensor networks"*, Nano Communication Networks, Vol. 1, No. 1, pp 3-19, March 2010.

[2] I.F. Akyildiz, J.M. Jornet and M.Pierobon, *"Nanonetworks: A New Frontier in Communications"*, Communications of the ACM, Vol. 54, No. 11, pp 84-89, November 2011.

[3] Q.H. Abbasi, K. Yang, N. Chopra, J.M. Jornet, N. A. Abuali, K.A. Qaraqe and A. Alomainy, *"Nano-Communication for Biomedical Applications: A Review on the State-of-the-Art From Physical Layers to Novel Networking Concepts"*, IEEE Access, Vol. 4, 2016.

[4] J.M. Jornet and I.F. Akyildiz, *"Graphene-Based Plasmonic Nano-antenna for Terahertz Band Communication in Nanonetworks"*, IEEE Journal on Selected Areas in Communications, Vol. 31, No. 12, December 2013.

[5] J.M. Jornet and I.F. Akyildiz, *"Channel Modeling and Capacity Analysis for Electromagnetic Wireless Nanonetworks in the Terahertz Band"*, IEEE Transactins on Wireless Communications, Vol. 10, No. 01, october 2011.

[6] H. Elayan, R. M. Shubair, J. M. Jornet, P. Johari, *"Terahertz Channel Model and Link Budget Analysis for Intrabody Nanoscale Communication"*, IEEE Transactions on Nanobioscience, Vol. 16, No. 6, September 2017

[7] C.S. Joseph, A.N. Yaroslavsky, V.A. Neel, T.M. Goyette and R.H. Giles *"Continouos wave terahertz transmission imaging of nonsmelanoma skin cancers"* Lasers Surgery Med., Vol. 43, No. 6, pp 457-462, 2011

[8] A. Goldsmith, *Wireless Communications*, Cambridge University Press, 2005.

[9] K. Yang, A. Pellegrini, M. O. Munoz, A. Brissi, A. Alomainy, and Y. Hao, *"Numerical Analysis and Characterization of THz Propagation Channel for Body-Centric Nano-Communications"*, IEEE Transactions on Terahertz Science and Technology, Vol. 5, No. 3, May 2015.

[10] Q.H. Abbasi, H. El Sallabi, N. Chopra, K. Yang, K.A. Qaraqe and A. Alomainy, *"Terahertz Channel Characterization Inside the Human Skin for Nano-Scale Body-Centric Networks"*, IEEE Transactions on Terahertz Science and Technology, Vol. 6, No. 3, May 2016.

[11] G. Piro, P. Bia, G. Boggia, D. Caratelli, L.A. Grieco and L. Mescia, *"Terahertz Electromagnetic Field Propagation in Human Tissues: A Study on Communication Capabilities"*, Journal of Nano Communication Networks, Vol. 10, pp 51-59, October 2016.

[12] K.M. Yaws, D.G. Mixon and W.P. Roach, *"Electromagnetic Properties of Tissue in the Optical region"*, Proc. of SPIE Vol. 6435, p 643507, February 2007.

[13] C.B. Reid, G. Reese, P.Gibson and A.P. Wallace, *"Terahertz Time-domain Spectroscopy of Human Blood"*, IEEE Journal of Biomedical and Health Informatics, Vol. 17, No. 4, July 2013.

[14] *"Blood Vessels"*, https://www.encyclopedia.com/medicine/anatomy-and-physiology/anatomy-and-physiology/blood-vessels Oxford University Press, 2001

[15] *"Layers of the Skin"*, https://training.seer.cancer.gov/melanoma/anatomy/layers.html, 2018-08-01

[16] K. Hwang, H. Kim, D.J. Kim, *"Thickness of skin and subcutaneous tissue of the free flap donor sites: A histologic study"* Microsurgery, Vol.36, No.1, pp.54-58, January 2016

[17] S.V. Hum, *"Half-wave Dipole"*, http://www.waves.utoronto.ca/prof/svhum/ece422/notes/07-halfwave.pdf, 2018-08-01

[18] N. Hasan, *"Tensorbundle Lab"*, https://tensorbundle.wixsite.com/home, 2018-08-14

[19] M. Heyden, J. Sun, S. Funkner, G. Mathias, H. Forbert, M. Havenith and D. Marx, *"Dissecting the THz spectrum of liquid water from first principles via correlations in time and space"*, Proc Natl Acad Sci U S Av.107(27), July 2010

[20] H. Elayan, P. Johari, R. M. Shubair, J. M. Jornet, *"Photothermal Modeling and Analysis of Intrabody Terahertz Nanoscale Communications"*, IEEE Transactions on Nanobioscience, Vol. 16, No. 8, December 2017.

A Code

A.1 Terahertz Channel Model Function

```
function THzChannelModel()

close all

% Initialization of constants and frequency conversions.
c = 299792458*10^3;
f = (0.5:0.1:1.5)*10^12;
lambda = c./f;
omega = 2*pi.*f;

% The model that should be simulated is extracted from the file
% LayeredModelData.txt where the depth and type of material is defined.
fileID = fopen('LayeredModelData.txt');
C = textscan(fileID,'%f %s');
fclose(fileID);

% The information from the model is put into different variables. The depth
% of the different layers could either be put directly into the data file
% or randomly generated according to values from "https://training.seer.
% cancer.gov/melanoma/anatomy/layers.html" and . Values is specified in the
% order of epidermis, dermis, blood and hypdermis.
c1 = 0.5;
c2 = 1.0;  %0.05-1.5 mm for epidermis.
c3 = 3.0;
c4 = 1.0;   %1.5-4 mm for dermis.
c5 = 0.5;
c6 = 0.5;   %0.1-1 mm for blood.
%c7 = 0.1;
%c8 = 1.4;   %0.1-1.5 mm for hypodermis.

c9 = c1+c2+c3+c4+c5+c6+0.1;
RandVar1 = ceil((c1 + c2*rand)*100)/100;
RandVar2 = ceil((c3 + c4*rand)*100)/100;
RandVar3 = ceil((c5 + c6*rand)*100)/100;

% Comment the first LayerDepth line for randomized values according to the
% above parameters (The randomized depths will round to the
% nearest 2 decimal points.) or comment the second LayerDepth to specify parameters
% in the LayeredModelData.txt file. The Type of layers have to be specified
% in the text file in either case.
%LayerDepth = C{1};
LayerDepth = [RandVar1; RandVar2; RandVar3; c9 - (RandVar1+RandVar2+RandVar3)];
LayerType = C{2};

% The cumulative sum of all previous layers determines at what distance
% each layer ends. The distance resolution is determined and the total
% distance of the simulation.
LayerEnd = cumsum(LayerDepth);
delta_d = 0.01;
dtot = sum(LayerDepth);

% The distance resolution has to be smaller than every depth of the layer.
if LayerDepth(:) < delta_d

    disp('Distance resolution is smaller than the depth of a layer, exiting')
    return;

end

% The permittivity of the current material is extracted from the
% function MaterialLibrary. The function uses the double debye equation or
% the Havrilak-Negami equation depending on the layer type. The parameters
% used for the calculations are stored in the library. The output is a
% vector containing the frequency dependent permittivity for all layers
% specified.
epsilon = MaterialLibrary(LayerType,omega);
```

```
% The relative permittivity is then converted into refractive index and
% divided into its real and imaginary parts.
n = sqrt(epsilon);
n_imag = imag(n);
n_real = real(n);

% The effective wavelength and absorption coefficient is determined for all
% layers.
lambda_Data = lambda./n_real';
mu_abs_Data = 4*pi.*n_imag'./lambda;

% The distance is divided up according to its resolution.
d = (delta_d:delta_d:dtot);

% Parameters for the first layer of simulation.
Layer = 1;
lambda_g = lambda_Data(Layer,:);
mu_abs = mu_abs_Data(Layer,:);

% The directivity of a narrow beam directional source with a gaussian beam
% pattern is calculated here, which has a range of 3 to 24 for angles of
% pi/2 to 0 respectively.
delta_theta = 78*pi/180;
Omega_A = (pi/2)*((8/3)-(cos(delta_theta)+cos(delta_theta)^2 +(1/3)*cos(delta_theta)^2));
D = 2.15; % This is now using the directivity of a half-wave dipole compared to a isotropic antenna.

%% Calculation of the losses

% This double loop calculates the spreading and absorption loss suffered
% from an electromagnetic wave traveling through some medium(s). It does it
% for all specified distances and frequencies.
for j = 1:length(d)

    % if the distance is greater then the distance at which the layer ends,
    % the values for effective wavelength and absorption coefficient will
    % be updated to match the new layer we've entered.
    if d(j) > LayerEnd(Layer) + delta_d/10 % delta_d/10 had to be added in order to remove a bug that cause

        Layer = Layer+1;
        lambda_g = lambda_Data(Layer,:);
        mu_abs = mu_abs_Data(Layer,:);

    end

    % This loop uses Frii's equation and Beer-Lamberts law to calculate the
    % spreading and absorption loss respectively.
    for i = 1:length(f)

        L_spr(j,i) = D.*((4.*pi.*d(j))./lambda_g(i)).^2;
        L_abs(j,i) = exp(mu_abs(i).*d(j));

    end

end

%% Re-structuring of the layered matrices.

% The previous calculations assume a homogenous medium, but since we have a
% layered structure we need to do some matching at the interface
% boundaries.

% The difference in a interface point will be stored in this variable,
% which is why it's set at ones initially since there will be no mismatch
% for the first layer.
Layer_Diff_Ref = ones(Layer,length(f));
Layer_Diff_Abs = ones(Layer,length(f));
Layer_Diff_Spr = ones(Layer,length(f));

% Here the difference between the last point in a layer and the first in
% the next get stored for all layers.
for i = 2:Layer
    for j = 1:length(f)
```

```
        Layer_Diff_Ref(i,j) = 1./(1-abs(((n_real(j,i-1)-n_real(j,i))/(n_real(j,i-1)+n_real(j,i)))).^2);
        Layer_Diff_Abs(i,j) = L_abs(uint16(LayerEnd(i-1)/delta_d),j)/L_abs((uint16(LayerEnd(i-1)/delta_d))+
        Layer_Diff_Spr(i,j) = L_spr(uint16(LayerEnd(i-1)/delta_d),j)/L_spr((uint16(LayerEnd(i-1)/delta_d))+

    end
end

R = Layer_Diff_Ref;

% For multiple layers this difference has to be stored as a cumulative
% product in order to produce continous results.
Layer_Diff_Ref = cumprod(Layer_Diff_Ref);
Layer_Diff_Abs = cumprod(Layer_Diff_Abs);
Layer_Diff_Spr = cumprod(Layer_Diff_Spr);

% The vector containing the differences between layers gets reproduced into
% different matrices depending on what layer suffers from what difference
% in this loop.
for i = 1:Layer

    Layer_Diff_Ref2 = repmat(Layer_Diff_Ref(i,:),uint16(LayerDepth(i)/delta_d),1);
    Layer_Diff_Abs2 = repmat(Layer_Diff_Abs(i,:),uint16(LayerDepth(i)/delta_d),1);
    Layer_Diff_Spr2 = repmat(Layer_Diff_Spr(i,:),uint16(LayerDepth(i)/delta_d),1);
    Layer_Diff_Ref_Mat(i) = {Layer_Diff_Ref2};
    Layer_Diff_Abs_Mat(i) = {Layer_Diff_Abs2};
    Layer_Diff_Spr_Mat(i) = {Layer_Diff_Spr2};

end

% The difference matrices corresponding to each layer finally get pieced
% together and multiplid with the original solution in order to produe a
% continous result.
E = vertcat(Layer_Diff_Ref_Mat{:});
A = vertcat(Layer_Diff_Abs_Mat{:});
B = vertcat(Layer_Diff_Spr_Mat{:});

L_abs2 = L_abs.*A;
L_spr2 = L_spr.*B;

% The total path loss is the product of the spreading and absorption loss.
L_tot = L_abs2.*L_spr2.*E;

% Creates a filename Data#.mat where the number is a persistent variable so
% every time the simulation is run it will save the data in a new file
% which makes creating a lot of data easier.
persistent number;
if isempty(number)
    number = 1;
end

filename = sprintf('Data%i.mat', number);
save(filename,'L_tot','LayerType','LayerDepth','L_abs2','L_spr2')

number = number + 1;

%% Plotting and visulization
% Uncomment for the plots you are interested in.

% A surface plot of the spreading path loss against frequency and distance.
figure
surf(f*10^-12,d,10*log10(L_spr2))
colormap('jet')
shading interp
title('Spreading Path Loss')
xlabel('Frequency (THz)')
ylabel('Distance(mm)')
zlabel('(dB)')

% A surface plot of the spreading path loss against frequency and distance
% without the matching at boundaries.
figure
surf(f*10^-12,d,10*log10(L_spr))
colormap('jet')
```

```
shading interp
title('Spreading Path Loss Without Boundary Matching')
xlabel('Frequency (THz)')
ylabel('Distance(mm)')
zlabel('(dB)')

% A surface plot of the absorption path loss against frequency and
% distance.
figure
surf(f*10^-12,d,10*log10(L_abs2))
colormap('jet')
shading interp
title('Absorption Path Loss')
xlabel('Frequency (THz)')
ylabel('Distance(mm)')
zlabel('(dB)')

% A surface plot of the absorption path loss against frequency and distance
% without the matching at boundaries.
figure
surf(f*10^-12,d,10*log10(L_abs))
colormap('jet')
shading interp
title('Absorption Path Loss Without Boundary Matching')
xlabel('Frequency (THz)')
ylabel('Distance(mm)')
zlabel('(dB)')

% The absorption coefficient for all layer types against frequency.
figure
plot(f*10^-12,mu_abs_Data')
title('Absorption Coefficient (mm^{-1})')
legend(LayerType{:})
xlabel('Frequency (THz)')

% The real part of the permittivity for all layer types against frequency.
figure
plot(f*10^-12,real(epsilon))
title('Permittivity (Real)')
legend(LayerType{:})
xlabel('Frequency (THz)')

% The imaginary part of the permittivity for all layer types against
% frequency.
figure
plot(f*10^-12,imag(epsilon))
title('Permittivity (Imaginary)')
legend(LayerType{:})
xlabel('Frequency (THz)')

% The reflection at interface boundaries displayed as a percentage of the
% total power. Will only be displayed if there is more than 1 layers since
% otherwise there is no interface boundaries.
if length(LayerType) > 1
    for k = 1:length(LayerType)-1

        legendtext{k} = sprintf('%s->%s', LayerType{k}, LayerType{k+1});

    end

    figure
    plot(f*10^-12,(R(2:end,:)-1)*100)
    title('Reflection at Interface Boundaries')
    legend(legendtext)
    ylabel('Reflection (%)')
    xlabel('Frequency (THz)')

end

% A surface plot of the total pathloss against frequency and distance.
figure
surf(f*10^-12,d,10*log10(L_tot))
title('Total Path Loss')
```

```
colormap('jet')
shading interp
xlabel('Freqency (THz)')
ylabel('Distance (mm)')
zlabel('(dB)')

end
```

A.2 Material Library Function

```
function [eps_rel] = MaterialLibrary(Type, omega)
% This function contains a library of parameters used to approximate the
% permittivity of different human tissues at the early terahertz band
% (0.1-1.5 THz). The function can as of now: the double relaxation debye
% equation and either the single or double Havrilak-Negami relaxation
% equation. The available human tissues found throughout different articles
% are as of now: Generic skin and blood, stratum corneum, epidermis, dermis
% and hypodermis.

% Values of the different relaxation parameters comes from these articles:
% Skin from ?Terahertz pulsed spectroscopy of human basal cell carcinoma?.
% Blood from "Terahertz Time-Domain Spectroscopy of Human Blood".
% Stratum Corneum, Epidermis, Dermis and Fat from Terahertz
% electromagnetic field propagation in human tissues: A study on
% communication capabilities.

% Allocation of space for the output and definition of the vacuum
% permittivity
eps_rel = zeros(length(omega),length(Type));
epsilon_0 = 8.854187817*10^-12;

% The loop runs for every type of layer that is specified in the input
% "Type"
for i = 1:length(Type)

    % The layer type get stored in a new variable that will be compared to
    % the predefined tissue types in the library. the variable index is
    % used to determine what kind of approximation will be used to
    % determine the permittivity.

    Layer = Type{i};
    index = 0;

    if strcmp(Layer,'Skin') == 1

        % Skin typically varies between 1.5 - 4 mm depending on where on
        % the body it is located.

        eps_inf = 3.024;
        eps_1 = 24.5544;
        eps_2 = 4.6954;
        tau_1 = 3.79*10^-12;
        tau_2 = 0.113*10^-12;

        index = 1;

    elseif strcmp(Layer,'Blood') == 1

        % The size of blood vessels varies enormously, from a diameter of
        % about 25 mm (1 inch) in the aorta to only 8 micrometer in the
        % capillaries. "https://www.encyclopedia.com/medicine/
        % anatomy-and-physiology/anatomy-and-physiology/blood-vessels"

        eps_inf = 2.1;
        eps_1 = 130;
        eps_2 = 3.8;
        tau_1 = 14.4*10^-12;
        tau_2 = 0.1*10^-12;

        index = 1;

    elseif strcmp(Layer,'StratumCorneum') == 1
```

```
        % The stratum corneum has a thickness between 10 and 40 micrometer.
        % "https://en.wikipedia.org/wiki/Stratum_corneum"

        alpha_1 = 1;
        beta_1 = 1;
        tau_1 = 15.9*10^-12;
        delta_eps_1 = 12.22;
        sigma = 0.035;
        eps_inf = 2.4;

        index = 2;

    elseif strcmp(Layer,'Epidermis') == 1

        % The thickness of the epidermis varies in different types of skin;
        % it is only .05 mm thick on the eyelids, and is 1.5 mm thick on
        % the palms and the soles of the feet. "https://training.seer.
        % cancer.gov/melanoma/anatomy/layers.html"

        alpha_1 = 0.95;
        beta_1 = 0.96;
        tau_1 = 15.9*10^-12;
        delta_eps_1 = 89.61;
        sigma = 0.01;
        eps_inf = 3;

        index = 2;

    elseif strcmp(Layer,'Dermis') == 1

        % The dermis is located beneath the epidermis and is the thickest
        % of the three layers of the skin (1.5 to 4 mm thick), making up
        % approximately 90 percent of the thickness of the skin.
        % "https://training.seer.cancer.gov/melanoma/anatomy/layers.html"

        alpha_1 = 0.92;
        alpha_2 = 0.97;
        beta_1 = 0.8;
        beta_2 = 0.99;
        tau_1 = 1.6*10^-12;
        tau_2 = 159*10^-9;
        delta_eps_1 = 5.96;
        delta_eps_2 = 380.4;
        sigma = 0.1;
        eps_inf = 4;

        index = 3;

    elseif strcmp(Layer,'Hypodermis') == 1

        % The thickness of the hypodermis ranged 1,913?7,105 ?m. The
        % hypodermis of the DIEP (7,105???4,543 ?m) was the thickest followed
        % by the ALT (6,012???4,092 ?m) and TD (4,688???1,905 ?m).
        % "Thickness of skin and subcutaneous tissue of the free flap donor
        % sites: A histologic study."

        alpha_1 = 1;
        alpha_2 = 0.89;
        beta_1 = 0.78;
        beta_2 = 0.90;
        tau_1 = 2.3*10^-12;
        tau_2 = 15.9*10^-9;
        delta_eps_1 = 1.14;
        delta_eps_2 = 9.8;
        sigma = 0.035;
        eps_inf = 2.5;

        index = 3;

    else

        disp('Material type could not be found, exiting')
```

```
        return;

    end

    if index == 1

        % This approximation uses the double Debye equations for 2
        % relaxation processes.

        eps_real = eps_inf + (eps_1-eps_2)./(1+(omega.*tau_1).^2) + (eps_2-eps_inf)./(1+(omega.*tau_2).^2);
        eps_imag = (eps_1-eps_2).*(omega.*tau_1)./(1+(omega.*tau_1).^2) + (eps_2-eps_inf).*(omega.*tau_2)./
        eps_rel(:,i) = complex(eps_real,eps_imag);

    elseif index == 2

        % This approximation uses the Havrilak-Negami equation for 1
        % relaxation process.

        phi = atan((((omega.*tau_1).^alpha_1)*sin(pi*alpha_1/2))/(1 + cos(pi*alpha_1/2*(omega.*tau_1.^alpha
        eps_real = eps_inf + delta_eps_1*((1 + 2*((omega.*tau_1).^alpha_1).*cos(pi*alpha_1/2) + (omega.*tau
        eps_imag = delta_eps_1*((1 + 2*((omega.*tau_1).^alpha_1).*cos(pi*alpha_1/2) + (omega.*tau_1).^(2*al
        eps_rel(:,i) = complex(eps_real,eps_imag);

    elseif index == 3

        % This approximation uses the Havrilak-Negami equation for 2
        % relaxation processes.

        phi_1 = atan((((omega.*tau_1).^alpha_1)*sin(pi*alpha_1/2))/(1 + cos(pi*alpha_1/2*(omega.*tau_1.^alp
        phi_2 = atan((((omega.*tau_2).^alpha_2)*sin(pi*alpha_2/2))/(1 + cos(pi*alpha_2/2*(omega.*tau_2.^alp
        eps_real = eps_inf + delta_eps_1*((1 + 2*((omega.*tau_1).^alpha_1).*cos(pi*alpha_1/2) + (omega.*tau
        eps_imag = delta_eps_1*((1 + 2*((omega.*tau_1).^alpha_1).*cos(pi*alpha_1/2) + (omega.*tau_1).^(2*al
        eps_rel(:,i) = complex(eps_real,eps_imag);

    end

end

end
```

A.3 Numerical Analysis Script

```
% This script uses the data generated by the terahertzpathlossmodel
% function to create a polynomial that approximates the path loss model of
% that function and can then be used to compare against many other such
% data sets.

close all
clear all
j = 1;

%Choose the data sets that will be used for the polynomial extraction.
for i=1:10

filename = sprintf('Data%i.mat', i);
load(filename);

%Frequency and distance declarations.
Depth(:) = LayerDepth(:);
delta_d = 0.01;
d = [0.01:0.01:sum(Depth)];
f = [0.5:0.1:1.5];

%Rearrangement of the arrays containing the relevant information in order
%to perform the multivariable polynomial extraction.
X = 10*log10(L_tot);
X = reshape(X,[uint16(sum(Depth)/delta_d)*length(f),1]);
d2 = repmat(d,length(f));
f2 = repelem(f,length(d))';
d2 = d2(1,:)';

%The polynomial extraction.
```

```
p = polyfitn([d2,f2],X,4);

%The polynomial coefficients is saved in another variable.
Coeff{j} = p.Coefficients;
j = j+1;

end

% This number should be sum(1:n+1) where n is the order of the polynom
Temp2 = zeros(1,15);

% This loop averages out all the polynomal coefficients calculated in the previous loop to create a new pol
for i=1:length(Coeff)

   Temp = Coeff{i};

   % This number should be sum(1:n+1) where n is the order of the polynom
   for j=1:15

       Temp2(j) = Temp2(j) + Temp(j);

   end

end

% The new coefficients replaces the old ones.
Temp2 = Temp2./length(Coeff);
p.Coefficients = Temp2;

%Evaluation in the same points as the data sets contain.
A = polyvaln(p,[d2,f2]);

%Re-structuring the 3d array of polynomial data.
Polynomial = reshape(A,[length(d),length(f)]);

% This loop compares the polynomial to a specific amount of data sets and
% computes the differences between the polynomial and those data sets.
for i = length(Coeff):100

    filename = sprintf('Data%i.mat', i);
    load(filename);
    Y = 10*log10(L_tot);
    DataSetLength(i) = length(Y);
    Diff(i) = sum(sum(abs(Polynomial(:,:) - Y(:,:))./Y(:,:)))/(length(d)*length(f));

end

MaxDataSetLength = max(DataSetLength);

% A figure showing the evaluation of the polynomial.
figure
surf(f,d,Polynomial)
shading interp
colormap ('jet')
title('Total Path Loss (Polynomial)')
ylabel('Distance (mm)')
xlabel('Frequency (THz)')
zlabel('(dB)')

% This figure shows the difference in % between the polynomial and the
% other data sets.
figure
plot(Diff(length(Coeff):end)*100)
title('Average Difference Between Polynomial And New Data Sets')
xlabel('Data Set')
ylabel('Average Difference (%)')

% This figure shows the difference in dB between the polynomial and the
% last data set used for comparison.
figure
surf(f,d(1:length(Y)),Polynomial(:,:) - Y(:,:))
shading interp
colormap('jet')
```

```
title('Total Path Loss Difference Between Polynomial And A Data Set')
ylabel('Distance (mm)')
xlabel('Frequency (THz)')
zlabel('(dB)')
```